Stereodynamics of *N*-Allyl-*N*-methyl-2-aminopropane. ^{1}H and ^{13}C{^{1}H} DNMR Studies. Molecular Mechanics Calculations

Jay H. Brown and C. Hackett Bushweller*

Department of Chemistry, University of Vermont, Burlington, Vermont 05405-0125

Received: February 5, 1997; In Final Form: May 16, 1997[⊗]

N-Allyl-*N*-methyl-2-aminopropane (AMAP) is a relatively simple tertiary amine that has a chiral center at the pyramidal nitrogen. Racemization occurs by inversion−rotation at nitrogen. For each AMAP enantiomer, conformational exchanges occur via isolated rotation about carbon−nitrogen and carbon−carbon bonds. The ^{1}H and ^{13}C{^{1}H} dynamic NMR (DNMR) spectra of AMAP show a higher temperature decoalescence due to slowing inversion−rotation at nitrogen ($\Delta G^{\ddagger} = 7.4$ kcal/mol at 162 K) and a more complex decoalescence at lower temperatures due to slowing isolated rotation about carbon−nitrogen bonds ($\Delta G^{\ddagger} = 5.1-5.5$ kcal/mol at 100−110 K). A well-defined ^{1}H NMR spectrum at 100 K is simulated accurately by invoking the presence of five equilibrium conformations including two conformers that interconvert rapidly at 100 K. A two-letter designation is used to name the various conformations. The first letter defines the orientation of the vinyl group with respect to the lone pair (G denotes gauche to the lone pair and to the N-methyl group; G′ denotes gauche to the lone pair and the isopropyl group; A denotes anti to the lone pair). The second letter defines the orientation of the isopropyl methine proton (G denotes gauche to the lone pair and to the N-methyl group; G′ denotes gauche to the lone pair and to the allyl group; A denotes anti to the lone pair). The major subspectrum at 100 K is assigned to a family of GG′ and G′G′ conformations (59 %) that interconvert rapidly at 100 K. Other subspectra at 100 K are assigned to the GG (36 %), GA (≈3 %), and AA (≈2 %) forms. The presence of dominant GG′, G′G′, and GG conformers is confirmed by the ^{13}C{^{1}H} NMR spectrum at 100 K. Conformational energies and internal rotation barriers calculated by using Allinger's MM2(87) molecular mechanics computer program show good agreement with the NMR data. AMAP shows stereodynamics very similar to *N*-ethyl-*N*-methyl-2-aminopropane.

Introduction

Tertiary aliphatic amines institute an important class of compounds. A complete understanding of the chemistry of such amines requires insight into the molecular stereodynamics. Interconversions among the equilibrium conformations of a tertiary aliphatic amine occur via isolated rotation about single bonds and via pyramidal inversion at nitrogen.[1−3] The overall inversion process is complex; it involves not only pyramidal inversion at nitrogen but also concomitant or accompanying rotation about carbon−nitrogen bonds.[1−4] It is best characterized as an *inversion−rotation* process. Isolated rotation barriers (no inversion) about carbon−nitrogen bonds in simple aliphatic amines are usually smaller than barriers to inversion−rotation at nitrogen.[1] The stereodynamics of many simple amines including methylamine,[5] dimethylamine,[5] trimethylamine,[5] ethylamine,[6] isopropylamine,[7] ethylmethylamine,[8] and dimethylethylamine[9] have been investigated by Raman, infrared, or microwave spectroscopy and molecular orbital theory. Barriers to pyramidal inversion have been measured in ammonia,[10] methylamine,[5a,11] dimethylamine,[5c] and trimethylamine.[12]

The combination of dynamic NMR (DNMR) spectroscopy[13] and molecular mechanics calculations[14] has been useful in studying the stereodynamics of more sterically encumbered tertiary aliphatic amines including diethylmethylamine,[15] triethylamine,[15,16] dibenzylmethylamine,[1] tribenzylamine,[17] isopropyldimethylamine,[18] isopropylethylmethylamine,[19] 2-butylethylmethylamine,[20] 2-(diethylamino)propane[21], 2-(dibenzylamino)propane[21], and a series of *tert*-butyldialkylamines.[4] In the *tert*-butyldialkylamines, the preferred route for exchange of the *tert*-butyl methyl groups among molecular sites is via concomitant *tert*-butyl rotation and nitrogen inversion.[4]

Steric crowding forces triisopropylamine into an equilibrium conformation that has essentially C_{3h} symmetry with an almost trigonal planar nitrogen atom and all three methine C−H bonds in the trigonal plane.[22] In sterically crowded systems such as $(CH_3CH_2)_2CHN(i\text{-}C_3H_7)_2$[23] and $(t\text{-}C_4H_9)_2CHN(CH_3)_2$,[24] there are significant barriers to isolated rotation about carbon−nitrogen bonds on an essentially trigonal planar nitrogen template. In *N*-neopentyl-4-*tert*-butylpiperidine, the unusual but nevertheless preferred conformation of the neopentyl group has the neopentyl *tert*-butyl group eclipsing the nitrogen lone pair.[25]

In some tertiary aliphatic amines that have relatively high symmetry, inversion−rotation is "DNMR-invisible".[1] Chirality induced by deuterium substitution in such amines has been used successfully to observe inversion−rotation that is otherwise DNMR-invisible.[26]

A number of factors will determine the relative energies of the equilibrium conformations of a tertiary aliphatic amine including the pyramidality at nitrogen and the steric and/or electronic requirements of various substituents.[1,2] In particular, previous studies of tertiary aliphatic amines showed that the methyl group of an N-ethyl substituent shows a strong, but not exclusive, preference for the position gauche to the nitrogen lone pair, as compared to the position anti to the lone pair.[15,16,19,21] The phenyl group on the N-benzyl substituent in tertiary aliphatic amines shows a conformational preference similar to methyl.[17,21] While the stereodynamics of allylamine have been studied by microwave spectroscopy,[27] by gas phase electron diffraction,[28] and by *ab initio* SCF calculations,[29] the conformational preference of the N-allyl substituent in a tertiary

* Corresponding author. FAX: 802.656.8705. Internet: cbushwel@zoo.uvm.edu

[⊗] Abstract published in *Advance ACS Abstracts,* July 1, 1997.

S1089-5639(97)00449-0 CCC: $14.00

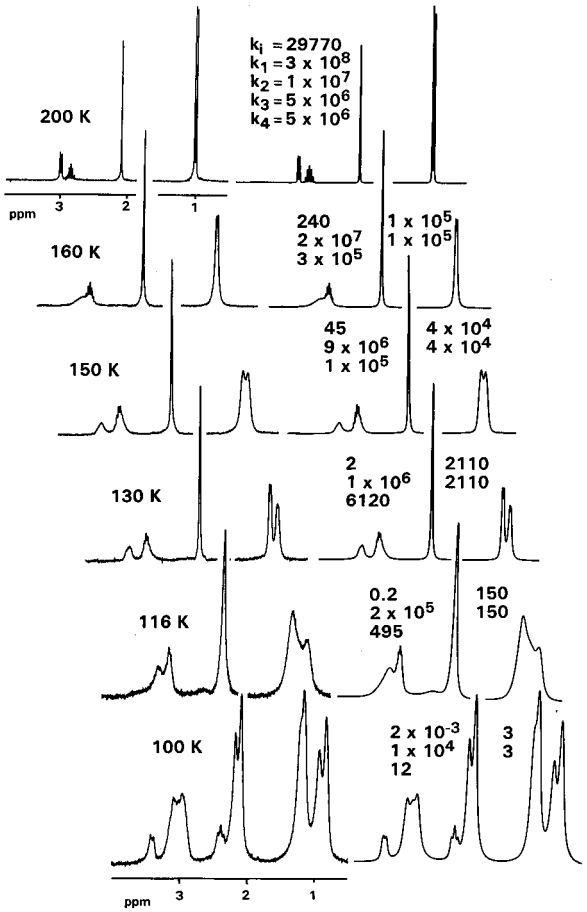

Figure 1. Experimental ^{1}H DNMR spectra (250 MHz) of the aliphatic protons of *N*-allyl-*N*-methyl-2-aminopropane (AMAP; 3 % v/v in $CBrF_3$) in the left column and theoretical simulations in the right column. Spectra are progressively offset to the left with increasing temperature. The rate constants k_1-k_4 are defined in Scheme 1; k_i is the rate constant for inversion−rotation at nitrogen.

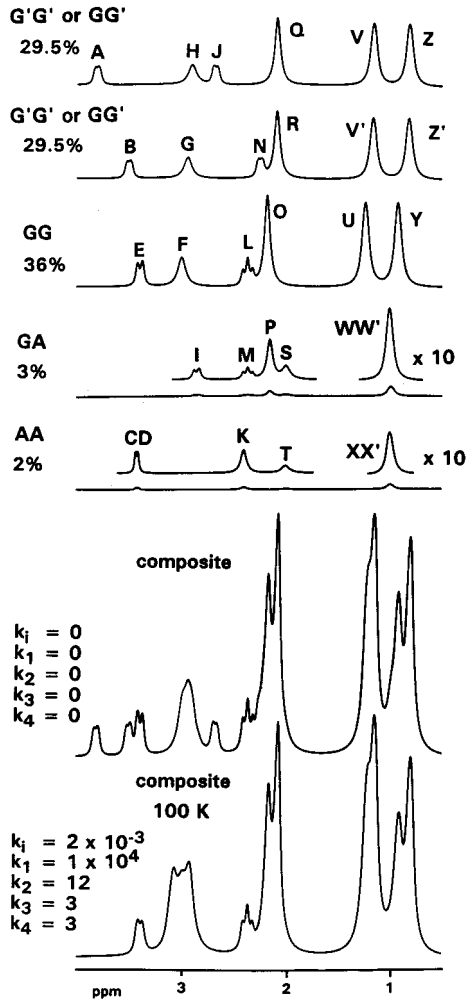

Figure 2. Subspectra invoked to simulate the ^{1}H NMR spectrum of the aliphatic protons of *N*-allyl-*N*-methyl-2-aminopropane (AMAP; 3 % v/v in $CBrF_3$) at 100 K. See Table 1 for a listing of chemical shifts.

amine has not been assessed. This paper reports ^{1}H and ^{13}C-{^{1}H} DNMR studies of *N*-allyl-*N*-methyl-2-aminopropane (AMAP). Inversion−rotation interconverts AMAP between enantiomers that respectively have R and S absolute configurations at nitrogen. For each enantiomer, there is a family of conformations that interconvert via isolated rotation about carbon−nitrogen bonds. This paper reports evidence for a strong preference for those conformations that have the isopropyl methyl groups respectively anti and gauche to the nitrogen lone pair with the vinyl group gauche to the lone pair. There is additional evidence for two minor conformations that have both isopropyl methyl groups gauche to the lone pair. Molecular mechanics calculations using the Allinger−Profeta amine force-field are in good agreement with experiment.[30]

DNMR Studies

The ^{1}H NMR spectrum (250 MHz) of AMAP (3 % v/v in $CBrF_3$) at 200 K shows a doublet at δ 1.00 ($^3J_{HCCH}$ = 6.1 Hz; $C(CH_3)_2$), a singlet at δ 2.10 (NCH_3), a septet at δ 2.84 ($^3J_{HCCH}$ = 6.1 Hz; NCH), a doublet of triplets at δ 2.98 ($^3J_{HCCH}$ = 6.7 Hz; $^4J_{HCCH=CH}$ = $^4J_{HCC=CH}$ = 1.2 Hz; NCH_2), and multiplets at δ 5.08 ($=CH_2$) and at δ 5.89 ($-CH=$). Below 170 K, decoalescence occurs. At 130 K, the signal due to the methylene protons is decoalesced into two resonances; the lower frequency (higher field) signal overlaps the methine proton resonance (Figure 1). At 130 K, the isopropyl methyl signal is decoalesced into two differentially broadened resonances (Figure 1). Using a well-established rationale, this decoalescence is assigned to slowing inversion−rotation at the pyramidal nitrogen.[1,19] At 130 K, inversion−rotation is slow on the NMR chemical exchange time scale, while all isolated rotations about carbon−carbon and carbon−nitrogen bonds remain fast.

Below 130 K, a second more complex decoalescence occurs due to slowing isolated rotation about the N−CH and N−CH_2 nitrogen−carbon bonds.[1,19] A resharpened spectrum is observed at 100 K (Figure 1). Accurate simulation of the 100 K spectrum can be achieved by invoking the five subspectra illustrated in Figure 2.[31] Superposition of the properly weighted subspectra produces the composite spectrum under conditions of no chemical exchange (second spectrum from bottom in Figure 2). The bottom composite spectrum in Figure 2 incorporates specific rates of chemical exchange that are necessary for an accurate simulation at 100 K.[19,21,31] Each and every methyl group resonance was simulated as three identical chemical shifts; that is, all isolated methyl rotations are fast at 100 K.

The spectrum at 100 K is dominated by two well-resolved subspectra; one accounts for 59 % of the total spectral area, the other 36 %. The 36 % subspectrum shows an NCH_3 singlet at δ_O 2.18, an unresolved isopropyl methine proton septet at δ_F 3.00 [efficient transverse relaxation (T_2*) and a small rate of chemical exchange obscure the $^3J_{HCCH}$ splitting], isopropyl methyl signals at δ_U 1.23 and δ_Y 0.92, and methylene protons signals at δ_E 3.40 ($^2J_{EL}$ = −12 Hz; $^3J_{HCCH} \approx$ 4 Hz) and δ_L 2.37 ($^3J_{HCCH}$ = 12 Hz). Based on established chemical shift trends, the isopropyl methyl resonance at δ_U 1.23 is assigned to a methyl group that is gauche to the nitrogen lone pair.[1,15,18,19,21] The isopropyl methyl signal at δ_Y 0.92 is assigned to a methyl group that is anti to the lone pair.[1,15,18,19,21] In the conformation

SCHEME 1: Stable Equilibrium Conformations of *N*-Allyl-*N*-methyl-2-aminopropane (AMAP): The Conformations Shown are Optimized Equilibrium Forms Computed by Using the MM2(87) Molecular Mechanics Force-Field[30]

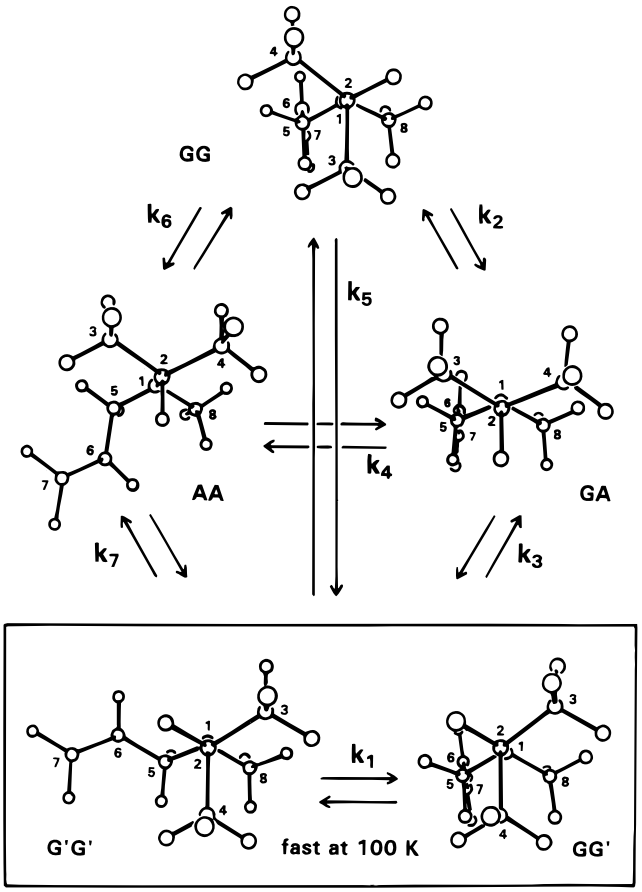

that gives this subspectrum, one isopropyl methyl group is gauche and the other anti to the lone pair. The chemical shift difference between the methylene protons ($\Delta\delta$ 1.03) is characteristic of NCH_2 protons that are "locked" in positions gauche and anti to the lone pair.[1,15,19,21,32] The resonance at δ_E 3.40 is assigned to a methylene proton that is gauche to the lone pair; the signal at δ_L 2.37 is due to a methylene proton that is anti to the lone pair. Based on the Karplus relationship between $^3J_{HCCH}$ and the HCCH torsion angle, the large $^3J_{HCCH}$ value (12 Hz) reveals that the methylene proton that is anti to the lone pair is also oriented anti to the vinyl methine proton.

The 36 % subspectrum is assigned to the GG conformer (Scheme 1).[33] In the GG form, the isopropyl methine proton and the vinyl group are both gauche to the lone pair and to the N-methyl group (G orientation).[33] The vinyl moiety is "locked" in the G position by the isopropyl methyl group that is gauche to the lone pair. This is reflected by the large chemical shift difference between the methylene protons ($\Delta\delta$ 1.03).[1,15,19,21,32] While isolated rotation about the $N-CH_2$ bond that interconverts GG and G′G forms (vinyl group passes lone pair) is expected to have a barrier lower than 4.5 kcal/mol (exchange is fast at 100 K),[15,16,19] any significant concentration of the G′G conformer is precluded by highly destabilizing syn-1,5-repulsions between isopropyl methyl and vinyl groups. Any exchange between the GG conformer and a minuscule concentration of the G′G conformer at 100 K will not result in any perceptible time-averaging of the methylene protons signals.[15,19] The large coupling of the vinyl methine proton to the methylene proton that is anti to the lone pair shows that these two protons prefer to be anti to each other, thus establishing the conformational preference of the vinyl group in the GG conformation. NMR parameters and conformational assignments are listed in Table 1.

The subspectrum that accounts for 59 % of the spectral area shows an NCH_3 singlet at δ 2.09, an isopropyl methine proton resonance at δ 2.92, and isopropyl methyl signals at δ 1.16 and δ 0.81. The isopropyl methyl resonance at δ 1.16 is assigned to a methyl group that is gauche to the nitrogen lone pair and that at δ 0.81 to a methyl group that is anti to the lone pair.[1,15,18,19,21] The isopropyl methyl chemical shifts reveal unequivocally that, in the conformation or conformations that give this subspectrum, one isopropyl methyl group is gauche and the other anti to the lone pair. Having assigned the 36 % subspectrum to the GG conformer, the 59 % subspectrum must be assigned to the GG′ or G′G′ conformer, *or* to a family of rapidly exchanging GG′ and G′G′ forms (Scheme 1).[1,15,19]

The methylene protons resonances in the 59 % subspectrum occur in a narrow range between 2.9 and 3.1 ppm. This is inconsistent with the presence of a single conformation (GG′ or G′G′) in which the methylene protons oriented anti and gauche to the lone pair whould show a large chemical shift difference.[1,15,19,21,32] The observed small chemical shift difference is consistent with the presence of a family of GG′ and G′G′ conformations that are exchanging rapidly at 100 K.[1,15,19] Exchange occurs by isolated rotation about the $N-CH_2$ bond with vinyl passing the lone pair. Molecular mechanics calculations (*vide infra*) predict that the isolated rotation barrier for interconversion between essentially isoenergetic GG′ and G′G′ conformations (vinyl passes lone pair) is a minuscule 2.8 kcal/mol. Consistent with this interpretation, an accurate theoretical simulation of the methylene protons signals at 100 K can be achieved by invoking exchange of magnetization between equally populated AJ (δ_A 3.82, δ_J 2.68, $^2J_{HCH} \approx -10$ Hz, $^3J_{HCCH}$ (J to vinyl methine proton) $\approx$ 4 Hz) and NB (δ_N 2.25, δ_B 3.51, $^2J_{HCH} \approx -10$ Hz, $^3J_{HCCH}$ (B to vinyl methine proton) $\approx$ 4 Hz) spin systems with a rate constant k_1 of 10^4 s^{-1} at 100 K (Figure 1). The methylene protons spectrum at 100 K reveals the onset of slowing exchange between GG′ and G′G′ conformations. The approximate free energy of activation is 3.8 kcal/mol at 100 K. The signals for the diastereotopic methyl groups fall, respectively, in narrow chemical shift ranges[1,15,18,19,21] and are not perceptibly affected at 100 K by the onset of slowing exchange between the GG′ and G′G′ conformations. Thus, the 59 % subspectrum is rationalized in terms of two subspectra that are undergoing rapid magnetization exchange at 100 K. The two subspectra employed in the composite theoretical simulations of the aliphatic region of the spectrum over a wide temperature range (Figure 1) are illustrated at the top of Figure 2. The various NMR parameters are compiled in Table 1.

After an exhaustive attempt to do so, the experimental ^1H DNMR spectra could not be simulated accurately over a wide temperature range by invoking only the three subspectra discussed above. A line-on-line fit could not be achieved at 100 K, and serious discrepancies could not be corrected at higher temperatures and higher rates of exchange. In a manner strictly analogous to that reported for *N*-ethyl-*N*-methyl-2-aminopropane,[19] accurate fits were achieved by invoking two additional minor subspectra. In one of the minor subspectra ($\approx$2 % at 100 K) internally consistent fits over a temperature range incorporated both methylene protons chemical shifts near δ 3.42 (both gauche to lone pair; *the vinyl group is anti to lone pair*) and both isopropyl methyl chemical shifts at δ 1.00. The presence of the methylene protons signals is manifested by a "distortion" (increased intensity) of the higher frequency component of the gauche methylene proton doublet at δ_E 3.40 and the GG conformer (Figure 1; 100 K). An *N*-methyl

TABLE 1: Conformational Assignments and Aliphatic Proton NMR Parameters Employed To Simulate the ^{1}H DNMR Spectra of AMAP[a]

	conformations[c]				
proton(s)[b]	GG (36 %)	G′G′ or GG′ (29.5%)	GG′ or G′G′ (29.5%)	GA (3%)	AA (2%)
$CH(CH_3*)_2$[d]	δ_U 1.23[e]	δ_V 1.16[e]	$\delta_{V'}$ 1.16[e]	δ_W 1.00[e]	δ_X 1.00[e]
	δ_Y 0.92[f]	δ_Z 0.81[f]	$\delta_{Z'}$ 0.81[f]	$\delta_{W'}$ 1.00[e]	$\delta_{X'}$ 1.00[e]
$CH*(CH_3)_2$[d]	δ_F 3.00	δ_H 2.90	δ_G 2.94	δ_S 2.00	δ_T 2.00
NCH_3	δ_O 2.18	δ_Q 2.09	δ_R 2.09	δ_P 2.16	δ_K 2.40
NCH_2	δ_E 3.40[e]	δ_A 3.82[e]	δ_B 3.51[e]	δ_I 2.86[e]	δ_C 3.42[e]
	$^2J_{EL} = -12$[g]	$^2J_{AJ} \approx -10$	$^2J_{BN} \approx -10$	$^2J_{IM} \approx -12$	$^2J_{CD} \approx -10$
	$^3J_{HCCH} \approx 4$	$^3J_{HCCH} \approx 4$	$^3J_{HCCH} \approx 4$	$^3J_{HCCH} \approx 4$	$^3J_{HCCH} \approx 4$
	δ_L 2.37[f]	δ_J 2.68[f]	δ_N 2.25[f]	δ_M 2.37[f]	δ_D 3.42[e]
	$^3J_{HCCH} = 12$	$^3J_{HCCH} \approx 4$	$^3J_{HCCH} \approx 4$	$^3J_{HCCH} \approx 11$	$^3J_{HCCH} \approx 4$

[a] 100 K in $CBrF_3$; TMS at 0.0 ppm. [b] Indicated by an asterisk. [c] See Scheme 1; see Figure 2 for a spectral decomposition at 100 K. [d] $^3J_{HCCH} = 6$ Hz. [e] Gauche to nitrogen lone pair. [f] Anti to nitrogen lone pair. [g] Hz.

TABLE 2: Relative Free Energies of the Stable Equilibrium Conformations of AMAP Determined by ^{1}H NMR Spectroscopy

conformation	relative free energy (kcal/mol)[a]
GG′/G′G′ family	0.0
GG	0.1
GA	0.6
AA	0.7

[a] At 100 K.

resonance at δ_K 2.40 (Table 1) was also invoked to achieve accurate fits of the spectral region near δ_L 2.37, i.e., near the GG anti methylene proton triplet (Figure 1). This subspectrum must be assigned to the AA conformation (Scheme 1). In the remaining subspectrum (≈3 % at 100 K), the chemical shifts invoked for the isopropyl methyl groups are identical at δ_W 1.00 and $\delta_{W'}$ 1.00. Methylene protons resonances were invoked at δ_I 2.86 (gauche to lone pair) and δ_M 2.37 (anti to lone pair) with a geminal coupling constant of about −12 Hz and a vicinal coupling of the anti proton to the vinyl methine proton of about 11 Hz. Invoking the methylene proton signal at δ_L 2.37 and the N-methyl resonance at δ_K 2.40 assigned to the AA conformer (*vide supra*) was required for accurate fits of the spectral region near δ_L 2.37, i.e., near the GG methylene proton triplet (Figure 1). The chemical shift difference between the methylene protons signals suggests methylene protons that are oriented anti and gauche to the lone pair. This subspectrum is logically assigned to the GA conformation (Scheme 1). In fact, the GA conformer is the only remaining stable conformation of AMAP that does not have destabilizing 1,5-repulsions between methyl or vinyl groups. It can be assigned by default. The estimated errors in measurement of all conformational populations is ±1 % at 100 K. Because the error in temperature measurement at these low temperatures is ±3 K and because it is not possible to measure conformer populations over a significant temperature range under conditions of slow exchange, no attempt was made to determine thermodynamic parameters ($\Delta H°$ and $\Delta S°$) for the various conformational equilibria. The relative *free energies* of the stable, NMR-detectable conformations at 100 K are compiled in Table 2.

All of the stable, equilibrium conformations of one invertomer of AMAP (S configuration at nitrogen) are illustrated in Scheme 1. The conformations in Scheme 1 interconvert by isolated rotation about carbon−nitrogen bonds with accompanying geometrical optimization of the vinyl group.

Theoretical simulations of the ^{1}H DNMR spectra over a wide temperature range allowed identification of the preferred pathways for conformational exchange in AMAP. The spectrum at 100 K is simulated accurately by invoking the five subspectra illustrated in Figure 2 with rapid exchange of magnetization at 100 K between the subspectra due to the G′G′ and GG′ conformations ($k_1 \approx 10^4$ s^{-1}). The approach used in simulating

TABLE 3: DNMR-Visible ^{1}H Magnetization Transfers Associated with Internal Rotation in AMAP

substituent	magnetization transfer[a]	rate constant (s^{-1})	conformational exchange[b]	$\Delta G^‡$ (kcal/mol)
$CH(CH_3)_2$	FUY to SWW′ (or SW′W)	k_2	GG to GA	5.1 ± 0.3[c]
	HVZ to SWW′ (or SW′W)	k_3	G′G′/GG′ to GA	5.5 ± 0.3[d]
	GV′Z′ to SWW′ (or SW′W)	k_3	G′G′/GG′ to GA	5.5 ± 0.3[d]
	SWW′ to TXX′ (or TX′X)	k_4	GA to AA	5.5 ± 0.5[d]
NCH_3	O to P	k_2	GG to GA	5.1 ± 0.3[c]
	Q to P	k_3	G′G′/GG′ to GA	5.5 ± 0.3[d]
	R to P	k_3	G′G′/GG′ to GA	5.5 ± 0.3[d]
	P to K	k_4	GA to AA	5.5 ± 0.5[d]
NCH_2	EL to IM	k_2	GG to GA	5.1 ± 0.3[c]
	BN to IM	k_3	G′G′/GG′ to GA	5.5 ± 0.3[d]
	AJ to MI	k_3	G′G′/GG′ to GA	5.5 ± 0.3[d]
	IM to CD (or DC)	k_4	GA to AA	5.5 ± 0.5[d]

[a] See Table 1 and Figures 1 and 2. [b] See Scheme 1. [c] At 100 K. [d] At 110 K.

the DNMR spectra was to start with the 100 K spectrum and, as the sample temperature increased, to turn on or increase only those rates that are necessary and sufficient to achieve accurate line shape simulations (Figure 1). The magnetization transfers used to simulate the DNMR spectra up to about 130 K, assigned conformational interconversions, and free energies of activation are listed in Table 3. Because the error in temperature measurement at these low temperatures is ±3 K and because the decoalescence phenomena occur over a relatively short temperature range, we hesitate to report $\Delta H^‡$ and $\Delta S^‡$ values for the rate processes detected. However, using the rate constants derived from the line shape simulations, $\Delta S^‡$ values for all processes are equal to 0 ± 3 cal/(mol K).

The primary internal motion associated with all of these DNMR-visible processes involves *isolated rotation* about carbon−nitrogen bonds (Scheme 1). As temperature increased, it was necessary to progressively increase the populations of the minor species. For example, the populations of the GA conformer are 4 % and 5 % at 115 and 130 K, respectively. The populations of the AA form are 3 % and 4 % at 115 and 130 K, respectively. Attempts to simulate the exchange-broadened DNMR spectra above 100 K without invoking the minor subspectra failed, providing strong circumstantial evidence for the presence of the minor conformations. In simulating the DNMR spectra, it was not necessary to invoke the k_5, k_6, k_7, and corresponding reverse processes (Scheme 1) to

achieve accurate fits of the spectra. It is apparent that the rates of these exchanges are sufficiently slower than the DNMR-detected processes (Table 3) that they do not affect the DNMR line shape.

Above 130 K, it became necessary to turn on random exchange among all N-methylene protons signals and among all isopropyl methyl protons resonances for all conformations. This reflects the onset of inversion−rotation and is associated with rate constant k_i in Figure 1 ($\Delta G^{\ddagger} = 7.4$ kcal/mol at 162 K).[1]

The preferred pathways for conformational exchange (via isolated rotation) involve the k_1-k_4 and reverse rate processes in Scheme 1. As described above, the barrier for the k_1 process is below the lower limit for accurate DNMR measurement in our laboratory (4.5 kcal/mol). The k_2-k_4 processes all involve *one* approximately 120° rotation about a carbon−nitrogen bond. During the k_4 conversion, vinyl must pass N-methyl and C−H bonds respectively pass the one pair and isopropyl group. The k_2 process involves C-methyl passing N-methylene, C−H passing N-methyl, and C-methyl passing the lone pair. The k_3 conversion (GG′ to GA) involves C-methyl passing N-methyl, C−H passing N-methylene, and C-methyl passing the loan pair. During all of these processes, at least one C−C bond must pass an N−C bond, leading to rotation barriers high enough to be DNMR-visible (5.1−5.5 kcal/mol).[15,16,18−21] The direct k_5 conversion (i.e., GG to GG′) must occur via a pathway that involves essentially two simultaneous C-methyl/N-methyl *and* C-methyl/N-methylene eclipsings. The GG to GG′ conversion can also occur via the GA form as an unstable intermediate; this requires two sequential 120° rotations, each of which involves just one C−C/N−C passing. Molecular mechanics calculations (*vide infra*) for AMAP predict a significantly higher barrier (8.4 kcal/mol) for the former process (k_5) than each of the latter sequential conversions (5.5 kcal/mol). The direct conversion is predicted to occur at a relative rate too slow to affect the DNMR line shape, as observed. Similar behavior is observed for *N*,*N*-dimethyl-2-aminopropane.[18] The k_6 and k_7 processes require two sequential 120° rotations and, for reasons of probability and possibly the intervention of highly unstable equilibrium conformations, occur at rates slower than the k_1-k_4 conversions. They do not perceptibly affect the DNMR line shape. Thus, the preferred exchange manifold for AMAP involves primarily a series of single 120° rotations about C−N bonds. For example, starting with the G′G′ form (Scheme 1), a preferred interconversion itinerary involves G′G′ going to GG′ to GA, which can proceed to either AA or GG. During all these processes, the vinyl group rotates to adopt an optimum equilibrium geometry. The family of GG′ and G′G′ conformations interconverts with the GG form via the less stable GA conformer as an intermediate.

In contrast to the isolated rotation barriers, the inversion−rotation barrier in AMAP is significantly higher at 7.4 kcal/mol.

The $^{13}C\{^1H\}$ NMR spectrum (62.9 MHz) of AMAP (3 % v/v in $CBrF_3$) at 210 K shows six singlets at δ 17.81 (isopropyl methyl carbons), δ 37.04 (N-methyl carbon), δ 53.58 (N-methylene carbon), δ 58.51 (isopropyl methine carbon), δ 117.97 (vinyl methylene carbon), and δ 138.32 (vinyl methine carbon). At 162 K, the resonance due to the prochiral isopropyl methyl groups is differentially broadened and almost decoalesced, while all other signals remain sharp (Figure 3). This is consistent with the onset of slowing nitrogen inversion while all isolated rotation processes remain fast.[1] Below 162 K, another decoalescence occurs and a sharpened spectrum is observed at 100 K (Figure 3). Simulation of the 100 K spectrum confirmed the presence of two dominant subspectra with

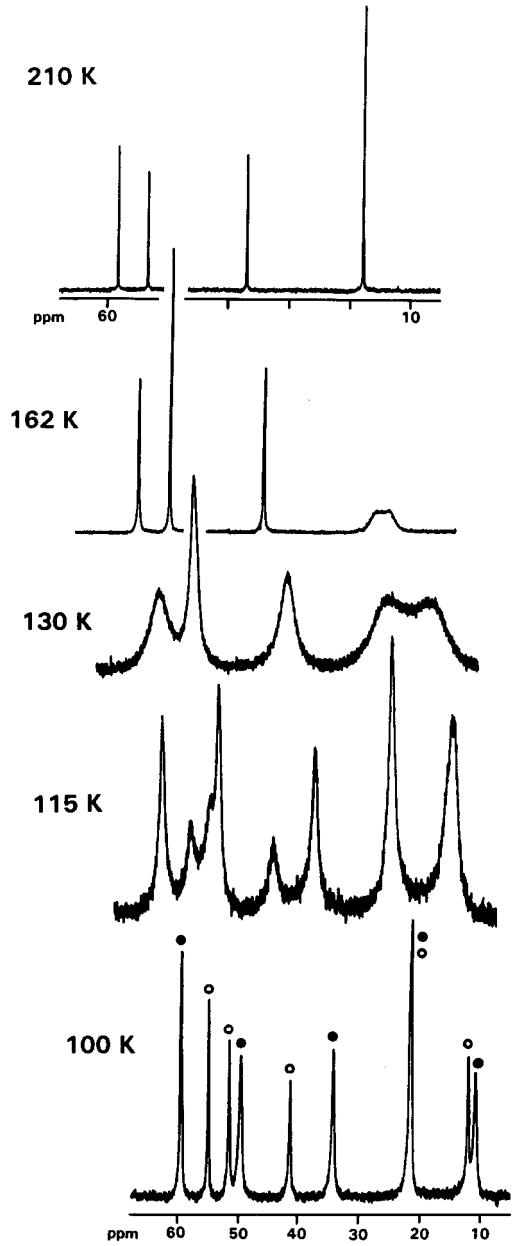

Figure 3. $^{13}C\{^1H\}$ DNMR spectra (62.898 MHz) of the aliphatic carbons of *N*-allyl-*N*-methyl-2-aminopropane (AMAP; 3 % v/v in $CBrF_3$). Spectra are progressively offset to the left with increasing temperature. The resonances at 100 K labeled with open circles are assigned to the GG conformation. The resonances labeled with solid circles are assigned to the family of rapidly interconverting GG′ and G′G′ conformations.

populations of approximately 65 % and 35 %. The 35 % subspectrum shows isopropyl methyl signals at δ 12.00 and 21.68 (methyl groups anti and gauche to lone pair[1,18,19,21]) and other resonances at δ 41.65, 51.89, 55.44, 119.05, and 139.91. These aliphatic carbon signals are labeled with open circles on the 100 K spectrum in Figure 3. Consistent with the analysis of the ^1H NMR spectrum at 100 K (*vide supra*), these signals are assigned to the GG conformation. The resonances due to the 65% subspectrum are labeled with solid circles on the 100 K spectrum in Figure 3. This subspectrum shows two isopropyl methyl signals at δ 10.77 and 21.68, revealing methyl groups that are respectively anti and gauche to the lone pair[1,18,19,21] and other resonances at δ 34.50, 49.42, 59.78, 118.76, and 138.95. These signals are logically assigned to the family of rapidly exchanging GG′ and G′G′ conformations. It is noteworthy that the signals in this subspectrum are broader than those in the 35 % subspectrum, consistent again with the onset of slowing

TABLE 4: Relative Energies of the Stable Equilibrium Conformations of AMAP Calculated by the MM2(87) Molecular Mechanics Force-Field

conformation	relative energy (kcal/mol)
GG′	0.00[a]
G′G′	0.07
GG	0.13
GA	0.21
AA	0.26

[a] $\Delta H_f = 0.30$ kcal/mol.

interconversion between the GG′ and G′G′ conformations (*vide supra*). There are no low-intensity signals observed that could be assigned to the GA or AA forms. Any such signals that are below 3 % the intensity of the major resonances could easily be lost in the noise on the 100 K spectrum. Improving the signal-to-noise on the 100 K spectrum was precluded by the danger to the magnet system of remaining at such a very low temperature for the required spectrum acquisition time. The ^{13}C NMR spectrum of AMAP does confirm the presence of dominant GG, GG′, and G′G′ conformations.

Molecular Mechanics Calculations

Molecular mechanics calculations based on the Allinger−Profeta amine force-field in the MM2(87) computer program agree with the stereodynamics deduced from the DNMR studies.[30] Five stable, equilibrium conformations were identified (Scheme 1). All five are predicted to be present at concentrations high enough to be NMR-detectable. For each stable form, the geometry was optimized by using the standard Newton−Raphson energy minimization scheme. MM2(87) predicts the GG′ conformation ($\Delta H_f = 0.30$ kcal/mol) to be most stable, with the G′G′ form only 0.07 kcal/mol less stable than GG′. The GG′ and G′G′ conformations are essentially isoenergetic. The GG, GA, and AA conformers are calculated to be 0.13, 0.21, and 0.26 kcal/mol, respectively, less stable than the GG′ form. The relative conformational energies are listed in Table 4. The GG′, G′G′, and GG conformations are predicted to be dominant, consistent with the ^1H DNMR data. Selected torsion angles, bond angles, and bond lengths are compiled in Table 5. In the GG′, G′G′, and GG conformers, MM2(87) predicts the torsion angle between the methylene proton that is anti to the lone pair and the vinyl methine proton to be 177°, 176°, and 177°, respectively. Based on the Karplus relationship for $^3J_{HCCH}$, the large, directly observed $^3J_{HCCH}$ coupling (12 Hz) between the N-methylene proton that is anti to the lone pair and the vinyl methine proton for the GG form is consistent with the MM2(87) calculation. Due to the rapid exchange between GG′ and G′G′ conformations, such $^3J_{HCCH}$ values cannot be measured directly for these species. In the GA form, the torsion angle between the methylene proton that is anti to the lone pair and the vinyl methine proton is calculated to be 178°. In the AA conformation, the torsion angle between the N-methylene proton that is proximate to the methyl group and the vinyl methine proton is calculated to be 172°.

It is reasonable to assume that the entropy difference between any two AMAP conformations will be small. At temperatures as low as 100 K, entropy contributions ($T\Delta S°$) to the free energy difference will be small. Therefore, the free energy differences compiled in Table 2 are good estimates of the enthalpy differences between conformers. While the NMR data do not allow an accurate measure of the relative free energies of the GG′ and G′G′ forms, there is no question that they are comparably populated. A perusal of Tables 2 and 4 shows good agreement between the conformational energies derived from the NMR data and those calculated by the MM2(87) force field.

TABLE 5: Selected Torsion Angles, Bond Angles, and Bond Lengths for the Stable, Equilibrium Conformations of AMAP Calculated by the MM2(87) Molecular Mechanics Force-Field

torsion angle (deg)		bond angle (deg)		bond length (Å)	
		GG′ Conformer[a]			
3-2-1-8	61.9	2-1-5	112.3	1-2	1.466
4-2-1-8	−64.3	2-1-8	113.7	1-5	1.461
2-1-5-6	160.7	5-1-8	110.2	1-8	1.456
1-5-6-7	121.0				
		G′G′ Conformer[a]			
3-2-1-8	64.0	2-1-5	113.0	1-2	1.467
4-2-1-8	−62.0	2-1-8	113.5	1-5	1.461
2-1-5-6	60.7	5-1-8	109.7	1-8	1.457
1-5-6-7	−121.1				
		GG Conformer[a]			
3-2-1-8	−66.6	2-1-5	114.0	1-2	1.466
4-2-1-8	167.2	2-1-8	112.0	1-5	1.460
2-1-5-6	165.1	5-1-8	110.2	1-8	1.458
1-5-6-7	120.4				
		AA Conformer[a]			
3-2-1-8	175.1	2-1-5	113.4	1-2	1.469
4-2-1-8	53.9	2-1-8	112.5	1-5	1.464
2-1-5-6	−59.7	5-1-8	110.6	1-8	1.458
1-5-6-7	117.0				
		GA Conformer[a]			
3-2-1-8	179.4	2-1-5	114.0	1-2	1.469
4-2-1-8	58.1	2-1-8	112.3	1-5	1.463
2-1-5-6	−60.8	5-1-8	109.8	1-8	1.459
1-5-6-7	−107.2				

[a] The atomic numbering scheme is given in Scheme 1.

TABLE 6: Selected Barriers to Isolated Rotation in AMAP Calculated by Using the Dihedral Driver Option in the MM2(87) Molecular Mechanics Force-Field

process[a]	barrier (kcal/mol)
G′G′ to GG′	2.79
GG′ to GA	5.56
GG to GA	5.49
GA to AA	4.55
GG to GG′	8.42

[a] The various conformations are illustrated in Scheme 1.

By using the general dihedral angle driver option in MM2-(87), isolated rotation barriers about nitrogen−carbon bonds in AMAP were calculated (Table 6). Consistent with the time-averaged character of the major ^1H NMR subspectrum of AMAP (Figure 2) and the presumption of rapid exchange between essentially isoenergetic GG′ and G′G′ conformations (vide supra), the MM2(87) barrier for direct interconversion of the GG′ and G′G′ conformations (vinyl passes lone pair) is a DNMR-invisible 2.79 kcal/mol. Those isolated rotations that involve methyl passing methyl (GG′ to GA) and methyl passing allyl (GG to GA) have MM2(87) barriers that are high enough to be DNMR-visible (Table 6). The GA to AA conversion (vinyl passes methyl) has a barrier that is calculated to be just above the lower limit for DNMR detection.[18] Consistent with the DNMR data, isolated rotations that involve CCH_3/NCH_3, CCH_3/NCH_2 or $CCH{=}CH_2/NCH_3$ eclipsings are predicted to be high enough to be DNMR-visible.

The stereodynamics of AMAP and *N*-ethyl-*N*-methyl-2-aminopropane (EMAP) and very similar.[19] The populations of dominant GG, GG′, and G′G′ conformations are comparable. The minor GA and AA forms are also present at comparable concentrations. Methyl and vinyl groups prefer to locate in the sterically less crowded position gauche to the lone pair and not in the sterically more crowded position anti to the lone pair. If one uses the *A*-value as a measure of the steric size of a substituent,[34] the similarity in stereodynamics for EMAP and AMAP is not surprising in light of the comparable *A*-values

for methyl (1.7 kcal/mol)[35] and vinyl (1.5−1.7 kcal/mol).[36] N-Ethyl and N-allyl substituents show very similar conformational preferences in analogous tertiary amines.

Experimental Section

NMR Spectra. The NMR spectra were recorded by using a Bruker WM-250 NMR system with a pole gap modified to allow safe operation (no magnet O-ring freezing) down to 93 K. NMR sample temperature was varied by using a custom-built cold nitrogen gas delivery system used in conjunction with the Bruker BVT-1000 temperature control unit. Temperature measurement is accurate to ±3 K. NMR samples were prepared on a vacuum line in precision 5 or 10 mm tubes and sealed after four freeze−pump−thaw cycles. All spectra are referenced to tetramethylsilane at 0 ppm.

***N*-Allyl-*N*-methyl-2-aminopropane (AMAP).** Allylamine (4.0 g, 0.07 mol) was added to a 500 mL three-neck round bottom flask equipped with a drying tube. Methanol (250 mL) was added to the flask. With cooling and stirring, acetone (8.2 g, 0.14 mol) and sodium cyanoborohydride (9.0 g, 0.14 mol) were added to the flask. The mixture was stirred at room temperature for 3 days. With cooling and stirring, the mixture was acidified to pH < 3 by using concentrated HCl (20 mL). The liquid was removed under vacuum. The resulting yellow residue was dissolved in 50 mL of water, and the mixture was washed with five 50 mL portions of diethyl ether. The aqueous layer was separated and added to a three-neck round bottom flask fitted with an efficient condenser. Diethyl ether (50 mL) was added to the flask. With cooling and stirring, solid KOH (15 g) was added to pH > 10. NaCl (5 g) was then added to the mixture. The mixture was stirred at room temperature for 24 h and filtered. The ether layer was separated, dried over Na_2SO_4 for 2 h, and filtered. The presence of *N*-allyl-2-aminopropane was confirmed by ^{1}H NMR. The solution of *N*-allyl-2-aminopropane in diethyl ether was added to a three-neck round bottom flask fitted with an efficient condenser. Formaldehyde (37 %; 11.5 g, 0.14 mol) was then added to the diethyl ether solution. With cooling and stirring, formic acid (97 %; 6.6 g, 0.14 mol) was added dropwise. The mixture was refluxed for 24 h. With cooling and stirring, concentrated HCl (10 g) was added. The bulk of the liquid was removed under vacuum leaving a wet orange solid amine hydrochloride. The amine hydrochloride was placed in a three-neck round bottom flask equipped with an efficient condenser. With cooling and stirring, the amine hydrochloride was neutralized by the slow addition of aqueous 40 % NaOH to pH > 10. The mixture was filtered. The top layer was separated and dried over Na_2SO_4 for 2 h. *N*-Allyl-*N*-methyl-2-aminopropane (AMAP) was purified on a 25 % SF-96/5 % XE-60 on Chromosorb W GLC column (20 ft × 3/8 in.) at 423 K. The structure of AMAP was confirmed by ^{1}H and ^{13}C NMR (see text) and mass spectrometry *m/e* (M+): 113.

Acknowledgment. C.H.B. is grateful to the National Science Foundation (Grant CHE80-24931) and to the University of Vermont Committee on Research and Scholarship for partial support of this research.

References and Notes

(1) For a recent review, see: Bushweller, C. H. In *Acyclic Organonitrogen Stereodynamics*; Lambert, J. B., Takeuchi, Y., Eds.; VCH Publishers: New York, 1992.

(2) For previous reviews, see: Lambert, J. B. *Top Stereochem.* **1971**, *6*, 19. Lehn, J. M. *Fortschr. Chem. Forsch.* **1970**, *15*, 311. Payne, P. W.; Allen, L. C. In *Applications of Electronic Structure Theory*; Schaefer, H. F., Ed.; Plenum Press: New York, 1977; Vol. 4. Rauk, A.; Allen, L. C.; Mislow, K. *Angew. Chem., Int. Ed. Engl.* **1970**, *9*, 400.

(3) Orville-Thomas, W. J., Ed. *Internal Rotation in Molecules*; J. Wiley and Sons: New York, 1974.

(4) Bushweller, C. H.; Anderson, W. G.; Stevenson, P. E.; Burkey, D. L.; O'Neil, J. W. *J. Am. Chem. Soc.* **1974**, *96*, 3892. Also see: Bushweller, C. H.; Anderson, W. G.; Stevenson, P. E.; O'Neil, J. W. *J. Am. Chem. Soc.* **1975**, *97*, 4338.

(5) (a) Tsuboi, M.; Hirakawa, A. Y.; Tamagake, K. J. *J. Mol. Spectrosc.* **1967**, *22*, 272. (b) Nishikawa, T.; Itoh, T.; Shimoda, K. *J. Am. Chem. Soc.* **1977**, *99*, 5570. (c) Wollrab, J. W.; Laurie, V. W. *J. Chem. Phys.* **1968**, *48*, 5058. (d) Erlandson, G.; Gurdy, W. *Phys. Rev.* **1957**, *10*, 513. (e) Lide, D. R.; Mann, D. E. *J. Chem. Phys.* **1958**, *28*, 572.

(6) Durig, J. R.; Li, Y. S. *J. Chem. Phys.* **1975**, *63*, 4110. Tsuboi, M.; Tamagake, K. J.; Hirakawa, A. Y.; Yamaguchi, J.; Nakagava, H.; Manocha, A. S.; Tuazon, E. C.; Fateley, W. G. *J. Chem. Phys.* **1975**, *63*, 5177.

(7) Krueger, P. J.; Jan, J. *Can. J. Chem.* **1970**, *48*, 3229.

(8) Durig, J. R.; Compton, D. A. C. *J. Phys. Chem.* **1979**, *83*, 2873.

(9) Durig, J. R.; Cox, F. O. *J. Mol. Struct.* **1982**, *95*, 85.

(10) Swalen, J. D.; Ibers, J. A. *Chem. Phys.* **1962**, *36*, 1914.

(11) Tsuboi, M.; Hirakawa, A. Y.; Takamitsu, I.; Sasaki, T.; Tamagake, K. J. *J. Chem. Phys.* **1964**, *41*, 2721.

(12) Weston, R. E., Jr. *J. Am. Chem. Soc.* **1954**, *76*, 2645.

(13) Oki, M. In *Applications of Dynamic NMR Spectroscopy to Organic Chemistry*; VCH Publishers: New York, 1985. Sandstrom, J. *Dynamic NMR Spectroscopy*; Academic Press: New York, 1982. Cotton, F. A. *Dynamic Nuclear Magnetic Resonance Spectroscopy*; Academic Press: New York, 1975.

(14) Burkert, U.; Allinger, N. L. *Molecular Mechanics*; American Chemical Society: Washington, DC, 1984. Allinger, N. L. *Adv. Phys. Org. Chem.* **1976**, *13*, 1.

(15) Bushweller, C. H.; Fleischman, S. H.; Grady, G. L.; McGoff, P.; Rithner, C. D.; Whalon, M. R.; Brennan, J. G.; Marcantonio, R. P.; Domingue, R. P. *J. Am. Chem. Soc.* **1982**, *104*, 6224.

(16) Fleischman, S. H.; Weltin, E. E.; Bushweller, C. H. *J. Comput. Chem.* **1985**, *6*, 249.

(17) Fleischman, S. H.; Whalon, M. R.; Rithner, C. D.; Grady, G. L.; Bushweller, C. H. *Tetrahedron Lett.* **1982**, 4233.

(18) Brown, J. H.; Bushweller, C. H. *J. Am. Chem. Soc.* **1992**, *114*, 8153.

(19) Brown, J. H.; Bushweller, C. H. *J. Phys. Chem.* **1994**, *98*, 11411.

(20) Danehey, C. T., Jr.; Grady, G. L.; Bonneau, P. R.; Bushweller, C. H. *J. Am. Chem. Soc.* **1988**, *110*, 7269.

(21) Brown, J. H.; Bushweller, C. H. *J. Am. Chem. Soc.* **1995**, *117*, 12567.

(22) Bock, H.; Coebel, I.; Havlas, Z.; Liedle, S.; Oberhammer, H. *Angew. Chem., Int. Ed. Engl.* **1991**, *30*, 187.

(23) Lunazzi, L.; Macciantelli, D.; Grossi, L. *Tetrahedron* **1983**, *39*, 305.

(24) Berger, P. A.; Hobbs, C. F. *Tetrahedron Lett.* **1978**, 1905.

(25) Forsyth, D. A.; Johnson, S. M. *J. Am. Chem. Soc.* **1993**, *115*, 3364.

(26) Forsyth, D. A.; Johnson, S. M. *J. Am. Chem. Soc.* **1994**, *116*, 11481.

(27) Roussy, G.; Demaison, J. *J. Mol. Spectrosc.* **1971**, *38*, 535. Botskor, I.; Rudolph, H. D. *J. Mol. Spectrosc.* **1974**, *53*, 15. Botskor, I.; Rudolph, H. D.; Roussy, G. *J. Mol. Spectrosc.* **1974**, *52*, 457. Botskor, I. *J. Mol. Spectrosc.* **1978**, *71*, 430.

(28) Hamada, Y.; Tsuboi, M.; Yamanouchi, K.; Matsuzawa, T.; Kuchitsu, K. *J. Mol. Struct.* **1990**, *224*, 345.

(29) Kao, J.; Seeman, J. I. *J. Comput. Chem.* **1984**, *5*, 200.

(30) Allinger, N. L. *QCPE* **1987**, Program No. MM2(87). Profeta, S., Jr.; Allinger, N. L. *J. Am. Chem. Soc.* **1985**, *107*, 1907.

(31) Brown, J. H.; Bushweller, C. H. *QCPE* **1993**, Program No. 633. For a PC-based program to plot the DNMR spectra, see: Brown, J. H. *QCPE* **1993**, Program No. QCMP 123.

(32) Hamlow, H. P.; Okuda, S. *Tetrahedron Lett.* **1964**, *37*, 2553. Lambert, J. B.; Keske, R. G.; Carhart, R. E.; Jovanovich, A. P. *J. Am. Chem. Soc.* **1967**, *89*, 3761.

(33) A two-letter designation is used to name the various conformations. The first letter defines the orientation of the vinyl group with respect to the lone pair (G denotes gauche to the lone pair and to the N-methyl group; G′ denotes gauche to the lone pair and to the isopropyl group; A denotes anti to the lone pair). The second letter defines the orientation of the isopropyl methine proton (G denotes gauche to the lone pair and to the N-methyl group; G′ denotes gauche to the lone pair and to the allyl group; A denotes anti to the lone pair).

(34) Bushweller, C. H. In *Conformational Behavior of Six-Membered Rings. Analysis, Dynamics, and Stereoelectronic Effects*; Juaristi, E., Ed.; VCH Publishers: New York, 1995.

(35) Anet, F. A. L.; Bradley, C. H.; Buchanan, G. W. *J. Am. Chem. Soc.* **1971**, *93*, 258. Booth, H.; Everett, J. R. *J. Chem. Soc., Perkin Trans. 2* **1980**, 255.

(36) Eliel, E. L.; Manoharan, M. *J. Org. Chem.* **1981**, *46*, 1959. Buchanan, G. W. *Can. J. Chem.* **1982**, *60*, 2908.